



Investigating the effects of land use change on flood hydrograph using HEC-HMS hydrologic model (case study: Ekbatan Dam)

Shahla Azizi¹ · Ali Reza Ilderomi¹ · Hamid Noori¹

Received: 30 November 2018 / Accepted: 29 May 2021 / Published online: 9 June 2021
© The Author(s), under exclusive licence to Springer Nature B.V. 2021

Abstract

Hydrological modeling academic studies have focused on the response to human-caused land use changes. The effects of land use change on flood degree in the catchment basin of Ekbatan Dam were investigated in this study, which looked at changes that occurred in 1985, 2000, and 2015. A combination of remote sensing and the Hydrologic Engineering Center-Hydrologic Modeling System (HEC-HMS) was used to achieve this goal. First, Landsat satellite images and sensors from Thematic Mapper, Enhanced Thematic Mapper Plus (ETM+), and Operational Land Imager were used to create land use maps for the target years. The weighted curve numbers (CN), a parameter related to infiltration, were then calculated for land uses. The extracted CN value, along with physiographic parameters and rainfall-runoff data, was then imported into the HEC-HMS model to simulate the effect of land use changes on runoff volume. After calibration and validation of the model using five (5) flood events, the simulation results showed an increase in the discharge peak volume of 64.3, 67.3, and 70.5 (m³/s) during the years 1985, 2000, and 2015, respectively, which resulted in an increase in the runoff height in these years as well.

Keywords Land use change · HEC-HMS model · Geographic information system · Flood hydrograph

1 Introduction

Floods are the most common natural disasters that cause human and financial losses (Shah et al. 2018; Vafakhah et al. 2020). Floods in Iran are primarily caused by natural-equilibrium disturbances such as land use changes and human intervention (Modarres et al. 2016;

✉ Ali Reza Ilderomi
a.ildoromi@yahoo.com

Shahla Azizi
shahlaazizi4@gmail.com

Hamid Noori
hamidwatershed@yahoo.com

¹ Department of Watershed Management, Faculty of Natural Resources, Malayer University, Hamadan, Iran

Peyravi and Marzaleh 2019; Yousefi 2020). Inconsistencies in land development capability and land use selection, as well as non-standard usage such as deforestation and subsequent increase in agricultural lands and urban development, result in higher discharge peak volume, increased flood occurrence, increased sediment, and erosion, all of which have negative environmental, economic, and social consequences (Calsamiglia et al. 2018; Llena et al. 2019; Sepehri et al. 2021). As a result, a better assessment of the effects of land use changes on flooding can be used as a powerful tool to reduce flood risk, which is one of the major issues in catchment planning, management, and sustainable development (Ali et al. 2011; Mustafa and Szydłowski 2020; Zuo et al. 2016). Hydraulic/hydrology models have become increasingly popular in recent years for assessing the impact of land use change on flooding severity. Dadhwal et al. (2010), for example, used VIC hydrological model to simulate the effect of land use changes in Mahanadi basin on rate of stream flow. Miller et al. (2002) used the Hydrologic Engineering Center-Hydrologic Modeling System (HEC-HMS) model to investigate the effects of land use change and vegetation on the hydrological responses of two United States (US) watersheds. In this regard, they prepared land use maps for these two basins at various intervals and in the forest, agriculture, urban areas, and bare lands classes. They concluded that from 1973 to 1997, the average annual runoff increased due to reduced forest area, agricultural land expansion, and urbanization.

Sajikumar and Remya (2015) used the Soil and Water Assessment Tool (SWAT) hydrologic model to investigate the effects of land use change on runoff parameters in India's Kerala watershed basin. The results showed that forestland decreased by 32%, resulting in a 15% increase in the watershed basin's discharge peak.

Brun and Band (2000) used Geographic Information Systems (GIS) and the Hydrological Simulation Program—FORTRAN (HSPF) to investigate the effects of land use change and urban development on the hydrologic behavior of the Glenfalls basin in the USA. According to the findings of this study, the change in land use resulted in a 20% decrease in base discharge flow. They also concluded that the severe impact threshold of urban development on the increase in runoff coefficient would be determined when 20% of the basin area is impenetrable.

Sanyal et al. (2014) investigated the impact of land use change in sub-basins on flood peak discharge at basin outlets in Eastern India. They began by preparing the land use maps for the 1976–2004 period using Landsat satellite images and ENVI software. They then investigated the effects of different land uses on the flood discharge peak using the HEC-HMS hydrologic model and the Natural Resources Conservation Service curve number (NRCS-CN) method.

Gao et al. (2020) used the HEC-HMS model to evaluate the effects of land use change on the hydrological responses of the drainage basin and discovered that the flood peak and volume in 2028 increased by about 3.5–2.9%, respectively, when compared to the flood peak and volume in 2010 in Qinhuai River Basin in the China.

Using the HEC-HMS model, Koneti et al. (2018) investigated the effects of land use change and vegetation on the hydrological responses of the Godavari River basin in India. According to the study, deforestation at the expense of urbanization and cropland expansion reduces overall evapotranspiration (ET) and infiltration while increasing runoff.

According to the studies cited, the effect of land use changes on runoff characteristics occurs locally. As a result, it is critical to assess the impact of land use change on runoff characteristics in the study area. Thus, the purpose of this study was to investigate the effects of land use change on flood hydrographs in Ekbatan Dam catchment basin during the years 1985, 2000, and 2015, using the HEC-HMS model, which is one of the most widely used hydrological models. The model for design flood estimation used some

transformation methods, the most well known of which are the Soil Conservation Service (SCS) unit hydrograph and the Snyder unit hydrograph. In the present study, the accuracy of flood estimation methods was evaluated, and the best method was used to assess the effect of land use changes on flooding degree.

2 Materials and methods

2.1 Description of the case study

The study area of the Ekbatan Dam basin is located in southeast of Hamadan province, Iran, at the “34° 34’”, “34° 45’” northern latitudes and “48° 42’”, “48° 28’” eastern longitudes (Fig. 1). This area is one of the Gharachai River’s sub-basins, located near Alvand Mountain to the southwest. The elevation map shows elevations ranging from 1948 to 3442 m above sea level. Based on Ekbatan Dam climatology data, the average annual rainfall and temperature are 343.11 mm and + 10.75 °C, respectively.

Thus far, studies show that land use change in Ekbatan Dam’s catchment area has influenced important hydrological parameters in the basin in recent decades. These parameters are as follows: 1. An increase in deposited sediments in the case study’s outlet (Ekbatan Dam) as a result of land plowing, 2. Reduction in extractable water resources as a result of flow coefficient reduction, resulting in: A. decrease in the volume of water behind the Ekbatan Dam, B. A case study of irrigated land drying, not utilizing the majority of the dam lake’s volume capacity, 3. Increase in spillway design flood as a result of increased flood potential caused by land use changes.

2.2 Required data

Different land uses were extracted from remotely sensed data to determine the hydrologic response to land use changes. Satellite images from the Thematic Mapper (TM), Enhanced

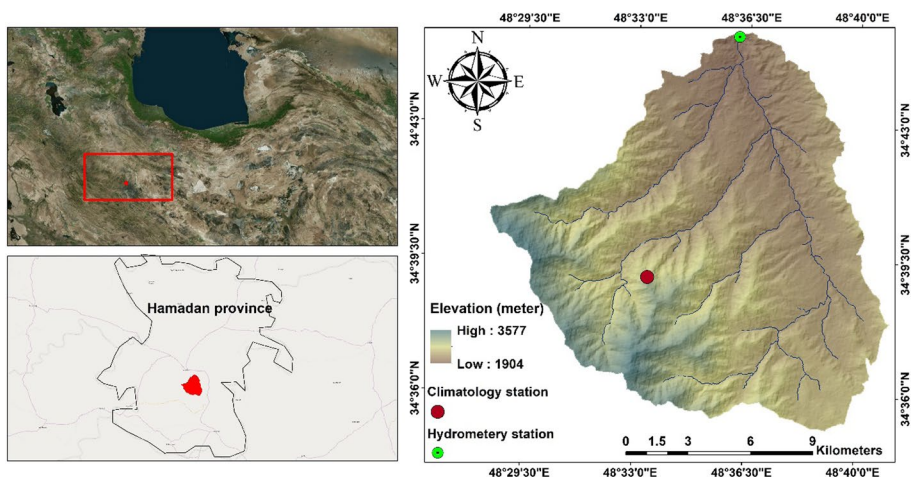


Fig. 1 Geographical location of the study area

Thematic Mapper Plus (ETM+), and Operational Land Imager (OLI) sensors, as well as the Landsat satellite, were used to assess land use patterns and their changes over time in 1985, 2000, and 2015. The images were obtained from the website of the United States Geological Survey (USGS) (<https://earthexplorer.usgs.gov/>) (Fig. 2). It was attempted to select images with high quality, that were cloud-free, and had a limited rate. Furthermore, in order to have a similar seasonal variation in land uses, the authors selected images that were taken during the same season, from July and September. In addition, all images processed with ENVI software were georeferenced and stacked to ensure clear images during the classification and accuracy assessment stages.

The land use classes of the desired years were merged, and six (6) new classes were created, namely rock outcrops, agriculture, residential, grass lands, water-covered, and dry farming. ENVI 4.5 software evaluated the accuracy of classified images from 1985, 2000, and 2015 using four (4) most popular factors, including total accuracy, kappa coefficient, manufacturer accuracy, and user precision, which were based on a comparison of the classified image and reference data, which accurately reflected the true land cover (Dissanayake et al. 2019; Lu and Weng 2007; Ranagalage et al. 2019). Meteorological, soil, and watershed characteristics were also required to simulate the rainfall-runoff process. The daily rainfall in Hamadan Province was obtained from the general meteorological office for 1985–2015. The observed discharge of events was obtained from the General Department of Natural Resources of Hamadan Province in order to calibrate and validate the data. In addition, the curve number (CN) as a soil infiltration agent was obtained from the General Department of Natural Resources of Hamadan Province. A digital elevation model (DEM) (scale 1: 25,000) was obtained from the Shuttle Radar Topographic Mission (SRTM) dataset to calculate watershed characteristics for HEC-HMS model inputs (using ArcGIS10.7 software) (such as lag time of the case study).

2.3 Detection of land use change

After developing land use maps using satellite imagery, the trend of different usage variations was studied over a thirty-year period. This analysis is extremely useful for management decisions in identifying and concluding that a class has been changed to other classes over a specified period of time (Chang and Franczyk 2008; Mustafa and Szydłowski 2020; Rahman 2016).

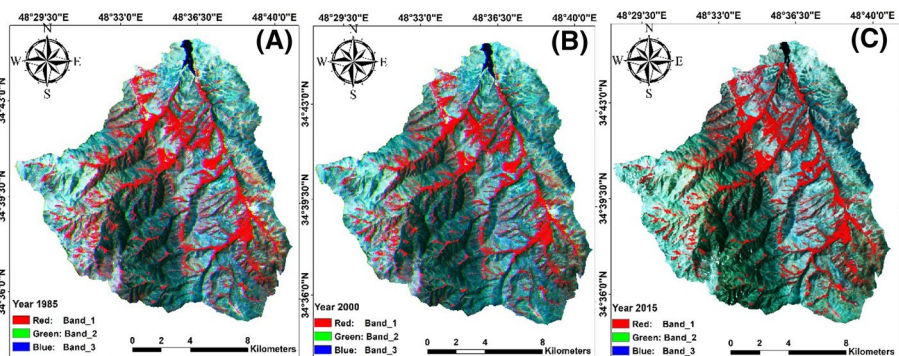


Fig. 2 Real images of each year by **a** TM1985 sensor, **b** ETM+ 2000 sensor, and **c** OLI 2015 sensor

2.4 HEC-HMS model

The US Army Corps of Engineers developed the HEC-HMS model, a semi-distributed and conceptually based model, to simulate the rainfall-runoff process in a watershed system. This model has been widely applied to the study of water resources, urban drainage systems, flood frequency, flood warning system planning, reservoir overflow design, and other topics (Gao et al. 2020; Sepehri et al. 2018, 2019). This model is run by a system of interconnected components, each of which simulates a different aspect of the rainfall-runoff process in a sub-basin or sub-area. In general, this model consists of three major components: the basin model, meteorological data analysis, and control specifications (Ali et al. 2011). A basin model is a graphical user interface that displays components of a hydrological system (such as stream length, elevation, and slope) and their interactive relationships. The SCS-CN method was used for runoff estimation due to its simplicity, flexibility, reliance on only CN, and acceptable accuracy (Halwatura and Najim 2013; Meresa 2019; Sepehri et al. 2018, 2019). The CN parameter is determined by the main characteristics of runoff generation, which include soil hydrological groups, basin land use (agriculture, forest, and urban), hydrologic status, and soil antecedent-moisture status (Mishra and Singh 2013). In this study, the constant monthly discharge method was used. The separator line of the base flow and direct runoff in this method begins at a point of minimum discharge from the onset of the flood runoff and continues in a straight line paralleled with the time axis until it cuts the falling limb (Rajkumar et al. 2021; Smakhtin 2001; Szilagyi and Parlange 1998).

Similar to Chen et al. (2009) and Malekinezhad et al. (2017), evapotranspiration (ET) losses were ignored due to the intensity of the storm event and the assumption that the ET volume is negligible in comparison with the runoff volume. For transformation, the SCS unit hydrograph and Snyder unit hydrograph methods were investigated, and the Muskingum–Cunge method was applied to routine river flow to basin outlet. HEC-HMS Technical Manual can be referred for more details on the model's description, as well as other options and parameters (USACE 2003).

2.4.1 Model calibration and validation

The sensitivity of the model to parameter change was investigated prior to calibration and validation of the used model. To this end, the results of the model curve variations were plotted for each of the input HEC-HMS model parameters. As the slope of the line rose, a small change in the desired parameter caused a large variation in the model's response, so the model is referred to as sensitive (Cunderlik and Simonovic 2004; Ouédraogo et al. 2018). In this study, three parameters were examined: lag time, CN, and initial abstraction (an empirical parameter for all losses prior to runoff calculated using CN). Following sensitivity analysis, a rainfall-runoff model was calibrated by selecting several flood events and changing the values of more sensitivity parameters within a reasonable range to match the simulated hydrograph to the observed hydrograph with the highest possible accuracy.

Following the completion of the calibration process, the model was validated with at least one more rainfall-runoff event. The model would be acceptable if it rebuilds the observed hydrographs of the hydrometric stations with acceptable accuracy and without changing the calibrated parameters (Katwal et al. 2021; Teng et al. 2018). Validation would continue until the best fit is found. Otherwise, because of the poor matching in the

validation process, the calibration process is repeated by changing the calibration parameters (Mandal et al. 2016; Roy et al. 2013). Three criteria were used to evaluate model performance accuracy: root-mean-square error (RMSE), coefficient of efficiency (CE), also known as the Nash–Sutcliffe coefficient, and R -square (R^2) (Eqs. 1–3).

$$\text{RMSE} = \sqrt{\frac{\sum (Q_o - Q_c)^2}{n}} \quad (1)$$

$$\text{CE} = 1 - \frac{\sum (Q_o - Q_c)^2}{\sum (Q_o - \bar{Q}_o)^2} \quad (2)$$

$$R^2 = \frac{[\sum (Q_o - \bar{Q}_o)(Q_c - \bar{Q}_c)]^2}{\sum (Q_o - \bar{Q}_o)^2 \sum (Q_c - \bar{Q}_c)^2} \quad (3)$$

where Q_c and Q_o are the estimated and observed hydrograph at the moment t . The larger value of RMSE, CE, and R^2 shows the higher model capability for simulations (Ali et al. 2011; Chen et al. 2009).

3 Results and discussion

Because of the effects on water resources, the hydrological response to human activity-induced land-cover changes in the Ekbatan Dam basin has received a lot of attention in recent years.

3.1 Land use map of Ekbatan Dam basin

The maximum likelihood method was used in the present study to calculate the classification accuracy of the produced land use change maps. The rate of accuracy was calculated by dividing the number of correctly classified reference points in a given class by the total number of reference points in that category. This ratio can be used as an omission error indicator (Mustafa and Szydlowski 2020; Story and Congalton 1986). The commission error was measured by the user's accuracy, which is the ratio of the number of correctly classified reference points of a specific class to the total number of points classified as that category (Fung and LeDrew 1988). The accuracy assessment for three images (TM (1985), ETM+(2000), and OLI (2015)) revealed an overall classification accuracy of more than 85%. Furthermore, the kappa coefficient computes the classification in comparison with a completely random classification. In this case, more accuracy is obtained than with an image that is classified completely randomly (Pontius et al. 2001; Story and Congalton 1986; Wu et al. 2019). The kappa coefficient has an advantage over overall accuracy in that it calculates accuracy using marginal (non-diagonal) elements of the error matrix (Mustafa and Szydlowski 2020). In this study, the calculated kappa coefficient using the maximum likelihood method was greater than 0.8. Different satellite images were used in the current study, and each image was analyzed and assessed separately (Table 1).

Table 1 Accuracy of classification coefficients using the maximum probability method

Landsat	Years	Kappa coefficient	Total accuracy	Grass-lands accuracy	Grass-lands producer accuracy	Agricultural use accuracy	Agricultural use producer accuracy	Residential use accuracy	Residential use producer accuracy	Dry farming use accuracy	Dry farming use producer accuracy	Rocky outcrop use accuracy	Rocky outcrop producer accuracy	Water-covered land use accuracy	Water-covered producer accuracy
TM	1985	0.88	90.37	74.27	96.27	97.3	97.3	79.33	86.86	75.93	75.93	100	91.91	100	94.19
ETM+	2000	0.83	86.59	62.45	98.72	100	95.89	84.51	87.59	81.76	81.76	100	58.16	100	94.23
OLI	2015	0.89	91.4	75	96.77	98.57	95.83	82.78	84.46	92.02	92.02	100	80.67	100	98.11

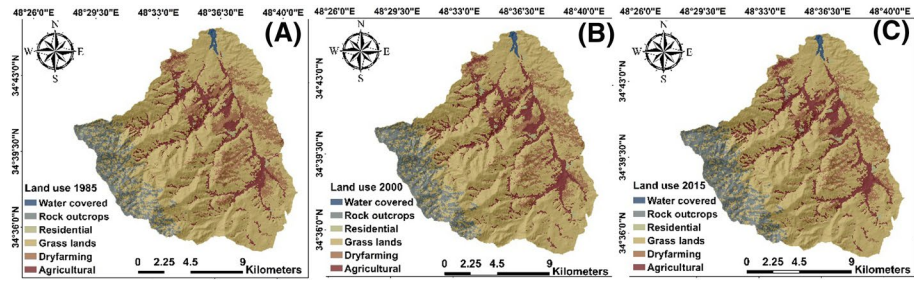


Fig. 3 Land use maps of the case study in **a** 1985, **b** 2000, and **c** 2015

Table 2 The area of total land use change in the target years

Land uses	Year 1985	Year 2000	Year 2015
	Area (km ²) (%)	Area (km ²) (%)	Area (km ²) (%)
Residential area	1.14 (31.64)	1.37 (0.61)	1.71 (0.76)
Dryland farming	24.61(157.89)	36.4 (16.31)	39.07 (17.68)
Agricultural lands	7.06 (0.91)	21.17 (9.49)	19.99 (8.8)
Grasslands	0.51(14.17)	156.34 (70.03)	154.51 (69.2)
Rocky outcrop	11.02 (70.74)	7.06 (3.16)	7.06 (3.16)
Water-covered lands	3.16 (0.4)	0.91 (0.4)	0.91 (0.4)

The rate of accuracy is determined by the quality of remote sensing data, which includes the resolution, available bands, and image quality (Alexakis et al. 2012; Iino et al. 2018; Jin-Song et al. 2009). There was a limitation in this study to examine the accuracy of classified maps due to the nature of land use changes, which vary depending on regional conditions, and also due to the lack of availability of ground values.

After developing land use maps using satellite imagery, the trend of different usage variations was studied over a thirty-year period. Figure 3 depicts each land use type and its changes over the specified time period.

The following is an explanation of land use change in the basin, based on Fig. 3 and Table 2: Residential use occupied 1.14 km² in 1985, accounting for 0.51% of the basin's total area; this would increase to 1.37 km² in 2000 (0.61%) and 1.71 km² in 2015 (0.76%). In 1985, grassland covered 157.89 km², accounting for 70.74% of the basin's total area. In 2000, the area of this use was 156.34 km² (70.03%), and it would be 154.51 km² in 2015. (69.2% of the total area of the basin). In 1985, agricultural lands and gardens covered 24.61 km², accounting for 11.02% of the basin's total area. This area would grow to 21.17 km² (9.49%) in 2000 and 20 km² (8.8% of the basin's total area) in 2015. In 1985, dry land farming covered 31.64 km², accounting for 14.17% of the basin's total area. It would reach 36.4 km² (16.31%) in 2000 and 39.07 km² (17.68% of the basin's total area) in 2015. In 1985, 2000, and 2015, the area of the rock outcrop without vegetation was 7.06 km², accounting for 3.16% of the basin's total area. Water-covered lands had an area of 0.91 km² in 1985, 2000, and 2015, accounting for 0.4% of the basin's total area.

3.2 Model sensitivity, calibration, and validation

In the case study, the values of each parameter were changed, and the results were analyzed at the basin outlet. The values of these three parameters were changed from -15% to $+15\%$ with a 5% interval, and the effects on flood peak discharge were studied. As shown in Tables 3, 4, 5, the model’s sensitivity to CN variations was high, so calibration processes were performed based on this parameter for four different flood events.

In the flood event of March 23, 2012, the observed and calculated peak discharges before calibration were 11.1 and $13.4 \text{ m}^3/\text{s}$, respectively, indicating a -20.7% error, and after calibration, the calculated peak discharge would be $10.9 \text{ m}^3/\text{s}$ (1.8% error), whereas in the Snyder method, the calculated peak discharge values before and after calibration were

Table 3 Results of model sensitivity to lag time

Parameter change	Lag time	Calculated peak discharge	Peak discharge variations	Sensitivity
15%	250.94	63.9	-0.62	-0.04
10%	240.09	64	-0.46	-0.03
5%	229.12	64.2	-0.15	-0.01
0	218.21	64.3	0	0
-5%	207.3	64.5	0.31	0.02
-10%	196.39	64.7	0.62	0.04
-15%	185.48	64.8	0.77	0.05

Table 4 Results of model sensitivity relative in proportion to initial abstraction

Parameter change	Initial abstraction	Calculated peak discharge	Peak discharge variations	Sensitivity
15%	13.29	63.7	-0.94	-0.06
10%	12.72	63.9	-0.62	-0.04
5%	12.15	64.1	-0.31	-0.02
0	11.58	64.3	0	0
-5%	11.01	64.7	0.62	0.04
-10%	10.44	4.9	0.93	0.06
-15%	9.87	65	1.08	0.07

Table 5 Results of model sensitivity to curve number (CN)

Parameter change	CN	Calculated peak discharge	Peak discharge variations	Sensitivity
15%	93.64	71.3	10.88	0.72
10%	89.57	68.1	5.9	0.39
5%	85.5	66.5	3.42	0.22
0	81.43	64.3	0	0
-5%	77.36	62.6	-2.71	-0.17
-10%	73.29	60.1	-6.98	-0.43
-15%	69.22	58.8	-9.35	-0.57

8.2 and 9.4 m³/s, respectively, with an error of 26.12 and 15.31% compared to the observed peak discharge (Fig. 4a–d).

In the case of April 17, 2001, the output of the SCS and Snyder methods before calibration was 6.8 and 10.1 m³/s, respectively, which, when compared to the observed peak discharge (8.4 m³/s), showed errors of 19.04 and –20.23%. The error of calculated discharges

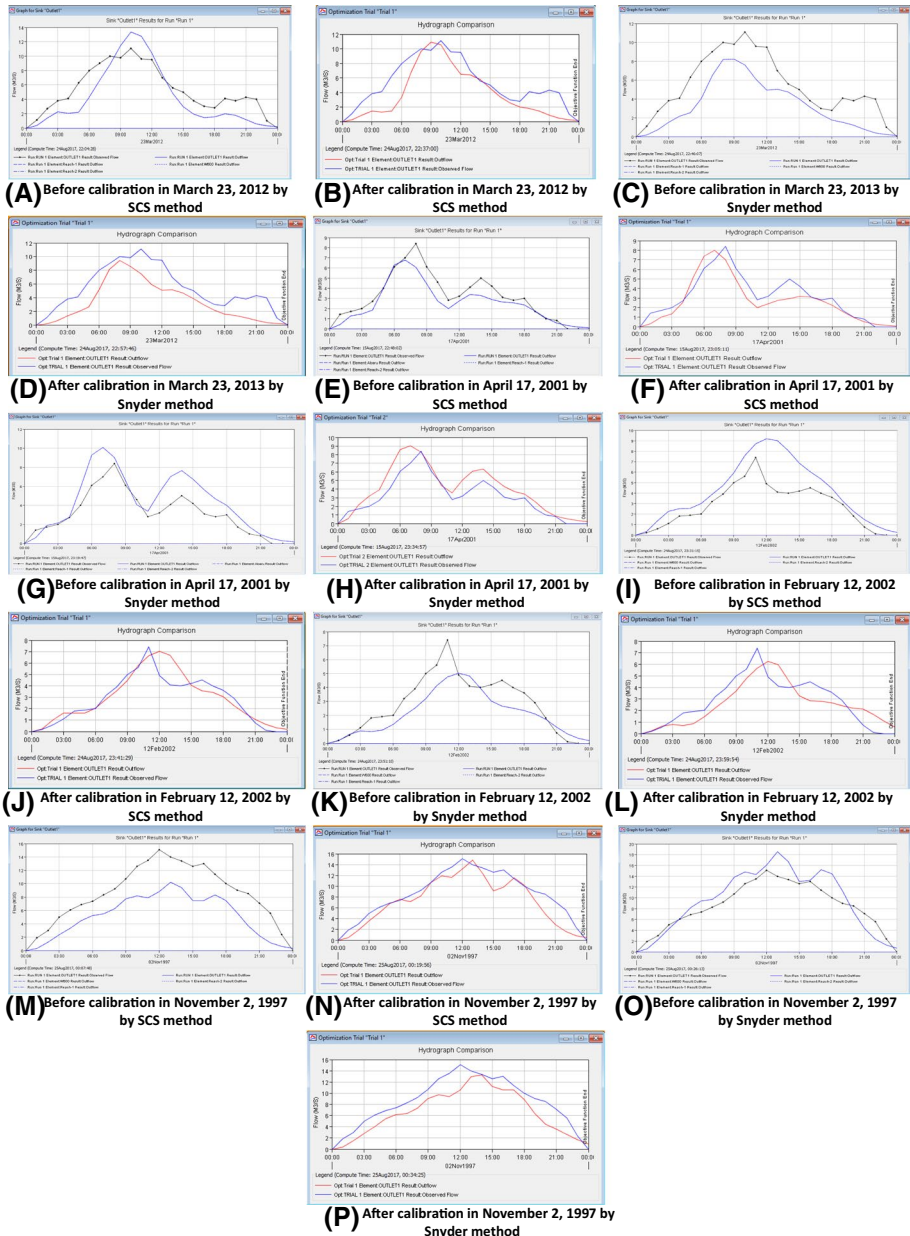


Fig. 4 Observed and calculated hydrograph for considered flood events

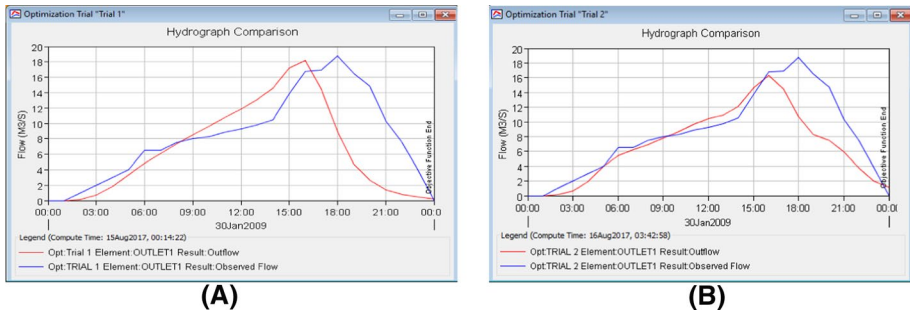


Fig. 5 Observed and calculated hydrograph in validation process of flood event of January 30, 2009 by **a** SCS and **b** Snyder methods

Table 6 Results of HEC-HMS model calibration and validation

Statistical index	R^2	CE	RMSE
Calibration	0.73	0.58	1.2
Validation	0.85	0.7	2.5

for SCS and Snyder methods would then be 4.76 and -8.33% , respectively, after the calibration process (Fig. 4e–h).

The observed and calculated peak discharge before calibration for February 12, 2002 event using the SCS method were 7.4 and 9.2 m³/s (-24.32% error), respectively, and 7.4 and 5 m³/s (32.43% error) using the Snyder method. After calibration, the calculated peak discharge in the SCS and Snyder methods was 7 and 6.3 m³/s, respectively (Fig. 4i–l). Furthermore, in the event of November 2, 1997, the performance of the SCS method in calculating the peak discharge before and after calibration was 32.45% and 1.9%, respectively, whereas these values for the Snyder method were -22.51% and 11.9%, respectively (Fig. 4m–p).

The calibration results for SCS and Snyder showed that both methods had acceptable accuracy in modeling the rainfall-runoff process, with the exception that the SCS unit hydrograph had more accuracy. On the other hand, the flood event of January 30, 2009 was used for validation, and the results showed that the SCS method outperformed the Snyder method (Fig. 5 and Table 6). As a result, the future analysis was based on the SCS unit hydrograph method.

3.3 Influence of land use change on flood hazard using HEC-HMS model

Flood hydrographs depicted the hydrological response to changes in land use, so land use maps for the case study were created using satellite images for the years 1985, 2000, and 2016 (Fig. 2). The extracted land uses were divided into six groups: grasslands, agricultural lands, dry land farming, residential lands, rock outcrops, and water-covered lands.

To calculate runoff, the SCS-CN loss method in the HEC-HMS model was investigated.

In this regard, the rainfall/runoff process was simulated using the weighted CN, which was calculated based on the type, area, and percent of various land uses (Table 2). The HEC-HMS model output for the first period of study (1985) revealed that the runoff

height and peak discharge of runoff are 283.72 mm and 64.3 m³/s, respectively (Fig. 6). The most common land uses at the time were grasslands, dry land farming, and agricultural lands. In next years, due to increased population and reduced water storages (Noori and Ilderomi 2013), the grasslands mainly were transferred to dry land farming and partly to residential areas, so that dry land farming and residential areas increased from 31.64 and 1.14 km² to 39.7 and 1.71 km², respectively. It is obvious that these transfers would increase the values of CN, which is a land use-related parameter, and thus the values of runoff volume and peak discharge. In this regard, the values of runoff height and peak discharge for the second period, i.e., 2000, were 453.19 mm and 67.3m³/s, respectively, indicating an increase of approximately 169.47 mm and 3 m³/s compared to the base period (i.e., 1985) (Fig. 7). Similarly, surveying the following and final period (2015) land uses revealed that this transferring continued. As a result, the runoff volume and height were higher in previous periods, at 494.71 mm and 70.5 m³/s, respectively (Fig. 8).

In a nutshell, decreasing the area of grasslands over time resulted in a significant increase in surface runoff. The increase in surface runoff was a result of a decrease in infiltration rate and, as a result, the process of groundwater recharge. Increased dry land farming and build-up areas as a result of population growth have resulted in an increase in land use changes. Increased dry land farming and development areas resulted in soil loss and, as a result, soil erosion. Soil erosion reduced either infiltration rate or terrain roughness, resulting in increased surface runoff. It should be noted that the occurrence of such changes is related to a small portion of the overall case study. The HEC-HMS

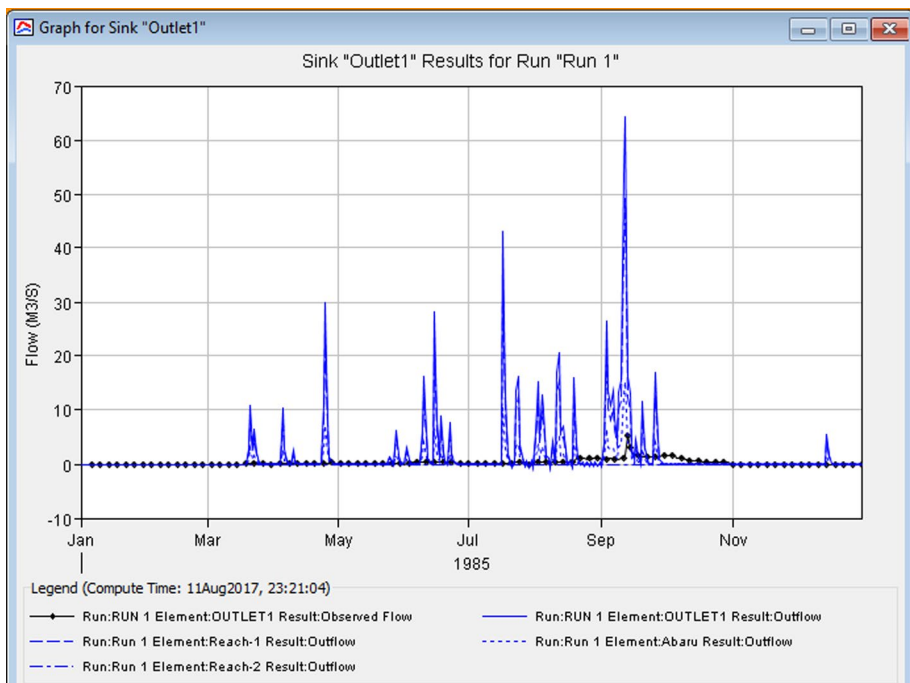


Fig. 6 Simulated daily discharge at the basin outlet in 1985

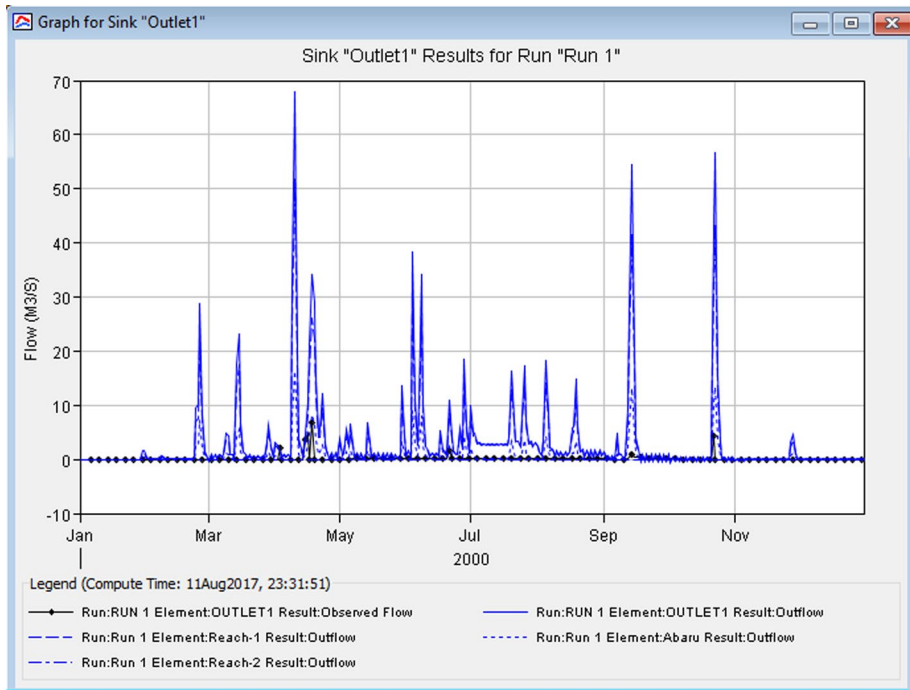


Fig. 7 Simulated daily discharge at the basin outlet in 2000

model can be used as a suitable means to simulate the role of land use scenarios and related concepts on hydrologic response at regional and global scales over the selected time frames.

4 Conclusion

Human life on Earth has resulted in enormous changes to the Earth's surface, such as the destruction of vast forests and pastures and the creation of dry agricultural lands; these factors have a significant impact on flood proneness. Land use changes and noncompliance with land ability are two of the most significant effects of human activity on flood occurrence (for cultivation). The effects of land use changes on basin hydrology include changes in peak discharge characteristics, total volume of runoff, water quality, and hydrologic equilibrium. Using flood hydrographs, the present study investigated the effects of land use change on the Ekbatan Dam basin in 1985, 2000, and 2015. The results revealed that there is a link between land use change and CN. The interaction of basin physical parameters in the HEC-HMS hydrologic model influenced their relationship with flood peak discharge in rainfall-runoff simulations. The effects of land use change are easily understood by examining CN, runoff, and flood peak discharge values. The simulation results for the target years (1985, 2000, and 2015) revealed that land use change during these intervals increased flood peak discharge, as well as runoff coefficient. As land use changes continue, grasslands and agricultural lands would decline, while dry lands would increase in the target

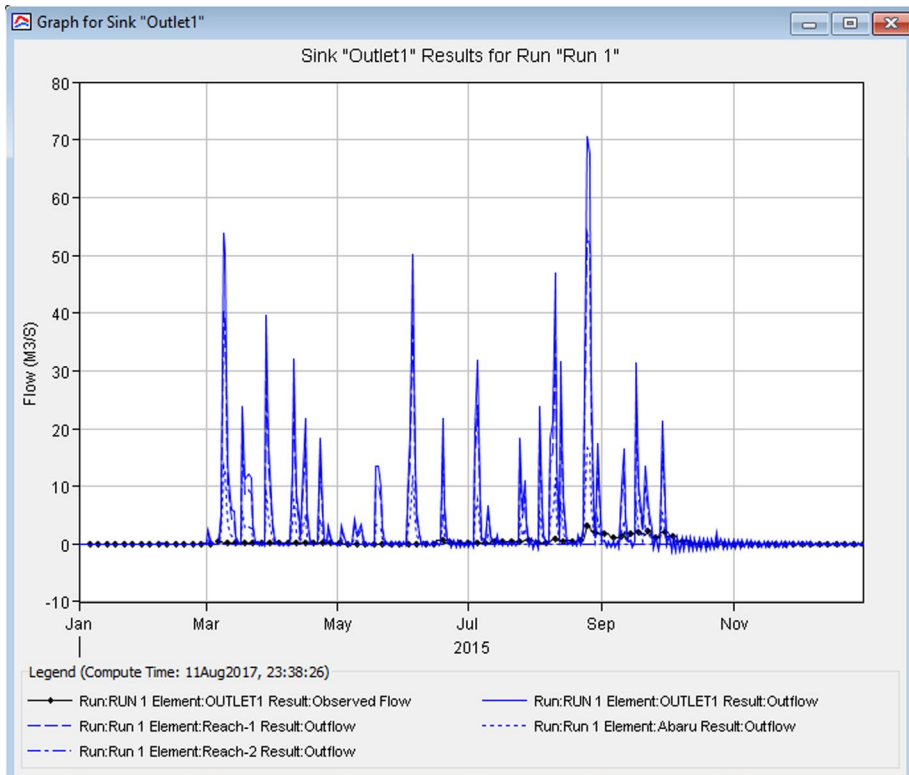


Fig. 8 Simulated daily discharge at the basin outlet in 2015

basin. As a result, it is expected that the basin will be more prone to flooding in the future, with increased runoff coefficient and peak discharge. The non-structural method can reduce peak discharge and flood volume in order to manage and reduce floods in the study area. As a result, in order to prevent flooding in the region, extending the dry lands by increasing gardens and agriculture, as well as managing the catchment basin's vegetation cover in the form of rangeland rehabilitation, can reduce peak discharge and runoff volume.

Declarations

Conflict of interest All authors declare that they have no conflict of interest.

References

- Alexakis DD, Agapiou A, Hadjimitsis DG, Retalis A (2012) Optimizing statistical classification accuracy of satellite remotely sensed imagery for supporting fast flood hydrological analysis. *Acta Geophys* 60:959–984
- Ali M, Khan SJ, Aslam I, Khan Z (2011) Simulation of the impacts of land-use change on surface runoff of Lai Nullah Basin in Islamabad Pakistan. *Landsc Urb Plan* 102:271–279
- Brun S, Band L (2000) Simulating runoff behavior in an urbanizing watershed. *Comput Environ Urb Syst* 24:5–22

- Calsamiglia A, Fortesa J, García-Comendador J, Lucas-Borja ME, Calvo-Cases A, Estrany J (2018) Spatial patterns of sediment connectivity in terraced lands: anthropogenic controls of catchment sensitivity. *Land Degrad Dev* 29:1198–1210
- Chang H, Franczyk J (2008) Climate change, land-use change, and floods: toward an integrated assessment. *Geogra Compass* 2:1549–1579
- Chen Y, Xu Y, Yin Y (2009) Impacts of land use change scenarios on storm-runoff generation in Xitiaoqi basin China. *Qua Int* 208:121–128
- Cunderlik J, Simonovic SP (2004) Calibration, verification and sensitivity analysis of the HEC-HMS hydrologic model. Department of civil and environmental engineering, The University of Western
- Dadhwal V, Aggarwal S, Mishra N (2010) Hydrological simulation of Mahanadi river basin and impact of land use/land cover change on surface runoff using a macro scale hydrological model. na
- Dissanayake D, Morimoto T, Ranagalage M, Murayama Y (2019) Land-use/land-cover changes and their impact on surface urban heat islands: case study of Kandy city Sri Lanka. *Climate* 7:99
- Fung T, LeDrew E (1988) For change detection using various accuracy. *Photogramm Eng Remote Sens* 54:1449–1454
- Gao Y, Chen J, Luo H, Wang H (2020) Prediction of hydrological responses to land use change. *Sci Total Environ* 708:134998
- Halwatura D, Najim M (2013) Application of the HEC-HMS model for runoff simulation in a tropical catchment. *Environ Model Softw* 46:155–162
- Iino S, Ito R, Doi K, Imaizumi T, Hikosaka S (2018) CNN-based generation of high-accuracy urban distribution maps utilising SAR satellite imagery for short-term change monitoring. *Int J Image Data fus* 9:302–318
- Jin-Song D, Ke W, Jun L, Yan-Hua D (2009) Urban land use change detection using multisensor satellite images. *Pedosphere* 19:96–103
- Katwal R, Li J, Zhang T, Hu C, Rafique MA, Zheng Y (2021) Event-based and continuous flood modeling in Zijinguan watershed Northern China. *Nat Hazards*. <https://doi.org/10.1007/s11069-021-04703-y>
- Koneti S, Sunkara SL, Roy PS (2018) Hydrological modeling with respect to impact of land-use and land-cover change on the runoff dynamics in Godavari River Basin using the HEC-HMS model. *ISPRS Int J Geo-Inf* 7:206
- Llena M, Vericat D, Cavalli M, Crema S, Smith M (2019) The effects of land use and topographic changes on sediment connectivity in mountain catchments. *Sci Total Environ* 660:899–912
- Lu D, Weng Q (2007) A Survey of Image classification methods and techniques for improving classification performance. *Int J Remote Sens* 28:823–870
- Malekinezhad H, Talebi A, Ilderomi AR, Hosseini SZ, Sepehri M (2017) Flood hazard mapping using fractal dimension of drainage network in Hamadan City Iran. *J Environ Eng Sci* 12:86–92
- Mandal A, Stephenson TS, Brown AA, Campbell JD, Taylor MA, Lumsden TL (2016) Rainfall-runoff simulations using the CARIWIG simple model for advection of storms and hurricanes and HEC-HMS: implications of Hurricane Ivan over the Jamaica hope river watershed. *Nat Hazards* 83:1635–1659
- Meresa H (2019) Modelling of river flow in ungauged catchment using remote sensing data: application of the empirical (SCS-CN), artificial neural network (ANN) and hydrological model (HEC-HMS). *Model Earth Syst Environ* 5:257–273
- Miller SN et al (2002) Integrating landscape assessment and hydrologic modeling for land cover change analysis I JAWRA. *J Am Water Resour Assoc* 38:915–929
- Mishra SK, Singh VP (2013) Soil conservation service curve number (SCS-CN) methodology vol 42. Springer Science & Business Media
- Modarres R, Sarhadi A, Burn DH (2016) Changes of extreme drought and flood events in Iran. *Global Planet Change* 144:67–81
- Mustafa A, Szydlowski M (2020) The impact of spatiotemporal changes in land development (1984–2019) on the increase in the runoff coefficient in Erbil Kurdistan Region of Iraq. *Remote Sens* 12:1302
- Noori H, Ilderomi AR (2013) The efficiency of geomorphology and geomorpho-climatology instantaneous unit hydrograph models in estimating flood discharges in Ekbatan of Hamedan watershed geospace 13: pp. 209–227
- Ouédraogo WAA, Raude JM, Gathenya JM (2018) Continuous modeling of the Mkurumudzi River catchment in Kenya using the HEC-HMS conceptual model: calibration, validation, model performance evaluation and sensitivity analysis. *Hydrology* 5:44
- Peyravi M (2019) Marzaleh MA (2020) the effect of the US sanctions on humanitarian aids during the great flood of Iran in. *Prehosp Disaster Med* 35:233–234
- Pontius RG Jr, Cornell JD, Hall CA (2001) Modeling the spatial pattern of land-use change with GEO-MOD2: application and validation for costa rica. *Agricu Ecosyst Environ* 85:191–203

- Rahman MT (2016) Detection of land use/land cover changes and urban sprawl in Al-Khobar Saudi Arabia: an analysis of multi-temporal remote sensing data. *ISPRS Int J Geo-Inf* 5:15
- Rajkumar S, Mishra S, Singh R (2021) Application of hydrologic modelling system (HEC-HMS) for flood assessment; case study of Kelani River Basin, Sri Lanka. In: Pandey A, Mishra SK, Kansal ML, Singh RD, Singh VP (eds) *Hydrological extremes*. Springer, Cham, pp 3–18
- Ranagalage M, Wang R, Gunarathna M, Dissanayake D, Murayama Y, Simwanda M (2019) Spatial forecasting of the landscape in rapidly urbanizing hill stations of South Asia: a case study of nuwara eliya, sri lanka (1996–2037). *Remote Sens* 11:1743
- Roy D, Begam S, Ghosh S, Jana S (2013) Calibration and validation of HEC-HMS model for a river basin in Eastern India. *ARPN J Eng Appl Sci* 8:40–56
- Sajikumar N, Remya R (2015) Impact of land cover and land use change on runoff characteristics. *J Environ Manage* 161:460–468
- Sanyal J, Densmore AL, Carboneau P (2014) Analysing the effect of land-use/cover changes at sub-catchment levels on downstream flood peaks: a semi-distributed modelling approach with sparse data. *CATENA* 118:28–40
- Sepehri M, Ghahramani A, Kiani-Harchegani M, Ildoromi AR, Talebi A, Rodrigo-Comino J (2021) Assessment of drainage network analysis methods to rank sediment yield hotspots. *Hydrol Sci J* 66(5):904–918
- Sepehri M, Malekinezhad H, Hosseini SZ, Ildoromi AR Suburban flood hazard mapping in Hamadan city, Iran. In: *Proceedings of the institution of civil engineers-municipal engineer, 2019*. Thomas Telford Ltd, pp 1–13
- Sepehri M, Malekinezhad H, Ilderomi AR, Talebi A, Hosseini SZ (2018) Studying the effect of rain water harvesting from roof surfaces on runoff and household consumption reduction. *Sustain Urb Areas* 43:317–324. <https://doi.org/10.1016/j.scs.2018.09.005>
- Shah AA, Ye J, Abid M, Khan J, Amir SM (2018) Flood hazards: household vulnerability and resilience in disaster-prone districts of Khyber Pakhtunkhwa province Pakistan. *Nat Hazards* 93:147–165
- Smakhtin V (2001) Estimating continuous monthly baseflow time series and their possible applications in the context of the ecological reserve. *Water Sa* 27:213–218
- Story M, Congalton RG (1986) Accuracy assessment: a user's perspective. *Photogramm Eng Remote Sens* 52:397–399
- Szilagyi J, Parlange MB (1998) Baseflow separation based on analytical solutions of the Boussinesq equation. *J Hydrol* 204:251–260
- Teng F, Huang W, Ginis I (2018) Hydrological modeling of storm runoff and snowmelt in Taunton River Basin by applications of HEC-HMS and PRMS models. *Nat Hazards* 91:179–199
- USACE, United States Army Corps of Engineers (2008) *Hydrological modeling system, HEC-HMS, user's manual, version 3.3*. Davis, CA, USA
- Vafakhah M, Loor MHS, Pourghasemi H, Katebikord A (2020) Comparing performance of random forest and adaptive neuro-fuzzy inference system data mining models for flood susceptibility mapping. *Arab J Geosci* 13:1–16
- Wu H, Li Z, Clarke KC, Shi W, Fang L, Lin A, Zhou J (2019) Examining the sensitivity of spatial scale in cellular automata Markov chain simulation of land use change. *Int J Geogr Inf Sci* 33:1040–1061
- Yousefi S et al (2020) Assessing the susceptibility of schools to flood events in Iran. *Sci Rep* 10:1–15
- Zuo D, Xu Z, Yao W, Jin S, Xiao P, Ran D (2016) Assessing the effects of changes in land use and climate on runoff and sediment yields from a watershed in the Loess Plateau of China. *Sci Total Environ* 544:238–250